Supplementary Information (SI) for Journal of Materials Chemistry A.

Supporting Information for

Bionic Liquid-Liquid Phase Separation Phenomenon Inspired Lignin Molecular Aggregates toward Highly Nitrogen-Doped Nanocarbon Anode for Sodium-Ion Hybrid Capacitors

Huiting Zhang[a,1], Wei Song[a,1,*], Zhenqiang Zhang[a], Jianhui Ma[a], Liheng Chen[a], Fangbao Fu[a], Xihong Zu[a], Dongjie Yang[b], Xueqing Qiu[a,c,d,e,*], Wenli Zhang[a,c,d,e,*]

[a]the Analysis and Test Center, Guangdong University of Technology, School of Chemical Engineering and Light Industry, Guangdong University of Technology (GDUT), Guangzhou, 510006, China

[b]School of Chemistry and Chemical Engineering, South China University of Technology, 381 Wushan Road, Tianhe District, Guangzhou, 510641, China

[c]Guangdong Provincial Laboratory of Chemistry and Fine Chemical Engineering Jieyang Center, Jieyang, 515200, China

[d]Shaoxing Research Institute of Renewable Energy and Molecular Engineering, Shanghai Jiao Tong University, Shaoxing, 312000, China

[e]Guangdong Basic Research Center of Excellence for Ecological Security and Green Development, Guangdong University of Technology, Guangzhou, 510006, China

*Corresponding authors.

E-mail address: songw@gdut.edu.cn (W. S.)

cexqqiu@scut.edu.cn (X.Q.Q.),

wlzhang@gdut.edu.cn (W.L.Z.)

[1] Huiting Zhang, and Dr. Wei Song contributed equally to this work.

1 Experimental Methods

1.1 Molecular Dynamic Simulation and Density Functional Theory Calculation

At first, we generated hundreds of initial configurations using the genmer module of the Molclus program. Then we pre-optimized all clusters using the semi-empirical method GFN2-Xtb. [1] The configurations obtained with low energy were further optimized, and their frequencies were calculated at the B3LYP-D3(BJ)/6-31G* level using the Gaussian16 package, taking into account an implicit solvent model. The interaction energy between the ammoxidized lignin (AOL) molecules and melamine-cyanuric acid (MCA) supermolecules and the energy among the AOL molecules, tannic acid (TA) molecules and MCA supermolecules were calculated with the correction of basis set superposition error (BSSE) at the B3LYP-D3(BJ)/6-311G** level. The Independent gradient model based on Hirshfeld partition (IGMH) [2] was analyzed by Multiwfn 3.8 (dev) program [3] and visualized with VMD 1.9.4. software [4] to investigate the weak interaction among the molecules.

2 Preparation of AOL

In the typical preparation process of ammonia-oxidized lignin (AOL)[5], 10 g of enzymatic hydrolyzed lignin (EHL) (Longli, Shangdong) was dispersed in 90 mL of 3% ammonia solution (Guangzhou Chemical Reagent Factory). Then, 10 mL of 30% hydrogen peroxide solution (Maclin) was added, and the mixture was stirred at room temperature for 10 min. Subsequently, the mixture was transferred into a hydrothermal reactor and reacted at 120 °C for 90 min. After the reaction was completed, the mixture was cooled to room temperature, and then the reaction product was subjected to rotary evaporation to remove the unreacted reactants and water, and then the product was vacuum-dried and ground into a powder.

2 Supporting Figures and Tables

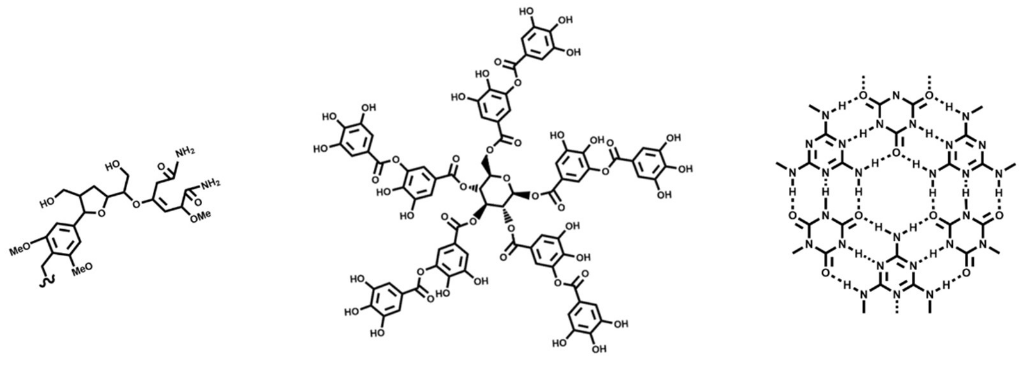

AOL TA MCA

Fig. S1. The chemical structures of AOL, TA, and MCA supermolecules.

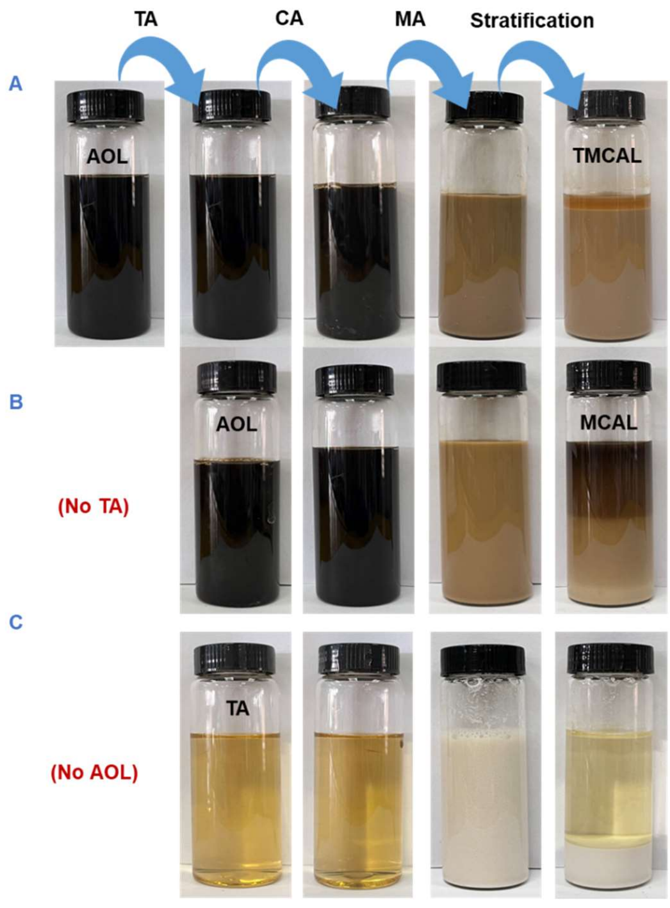

Fig. S2. Optical photos of solution states in comparative experiments.

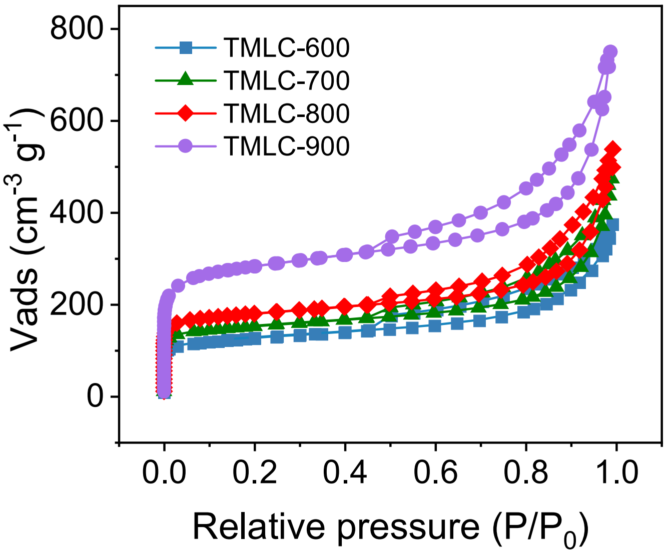

Fig. S3. N_2 adsorption/desorption isotherms of TMLCs.

Table S1 Porosity parameters of TMLCs samples.

Sample	S_{BET} ($m^2\ g^{-1}$)	V_{Total} ($cm^3\ g^{-1}$)	V_{micro} ($cm^3\ g^{-1}$)	V_{meso} ($cm^3\ g^{-1}$)	V_{micro}/V_{total} (%)	D_{ave} (nm)
TMLC-600	417	0.35	0.11	0.19	32.88	5.56
TMLC-700	497	0.47	0.15	0.25	30.91	5.90
TMLC-800	579	0.65	0.20	0.41	30.81	4.89
TMLC-900	933	0.67	0.27	0.30	40.93	4.98

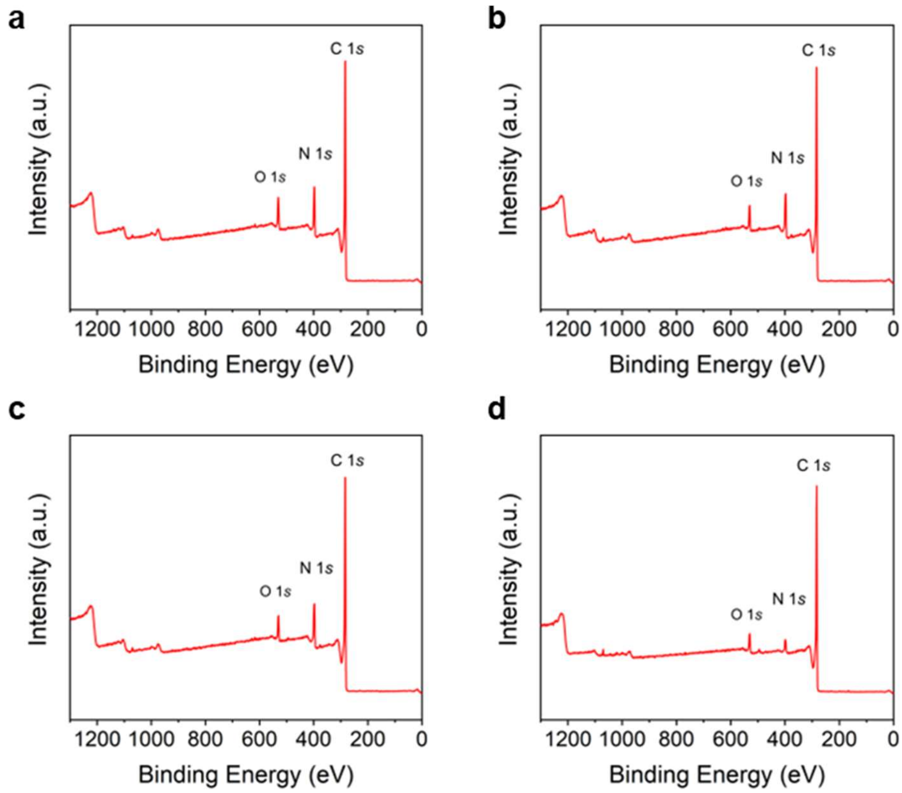

Fig. S4. XPS spectra of the (a) TMLC-600, (b) TMLC-700, (C) TMLC-800 and (d) TMLC-900.

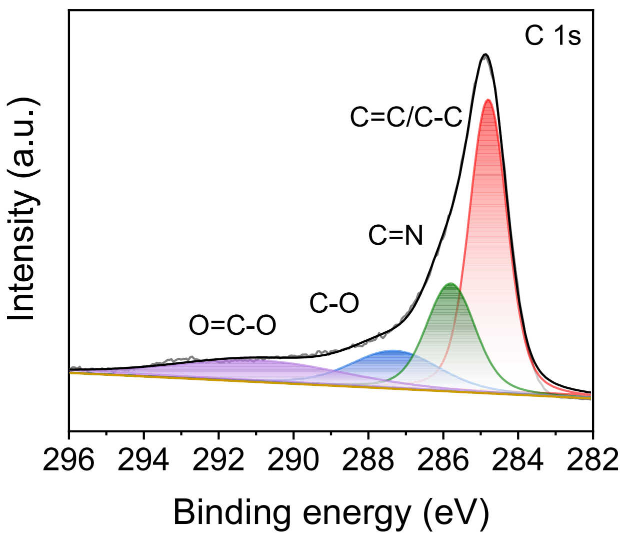

Fig. S5. High-resolution C 1s XPS spectrum of the TMLC-700.

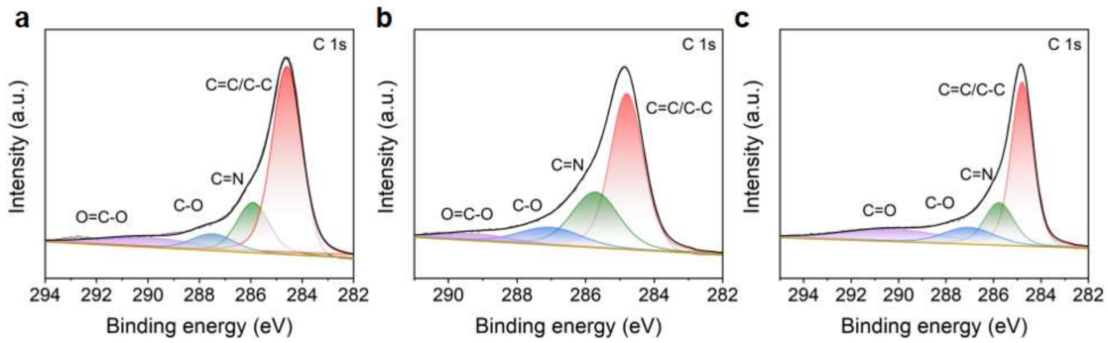

Fig. S6. High-resolution C 1s XPS spectra of (a) TMLC-600. (b) TMLC-800 (C) TMLC-900.

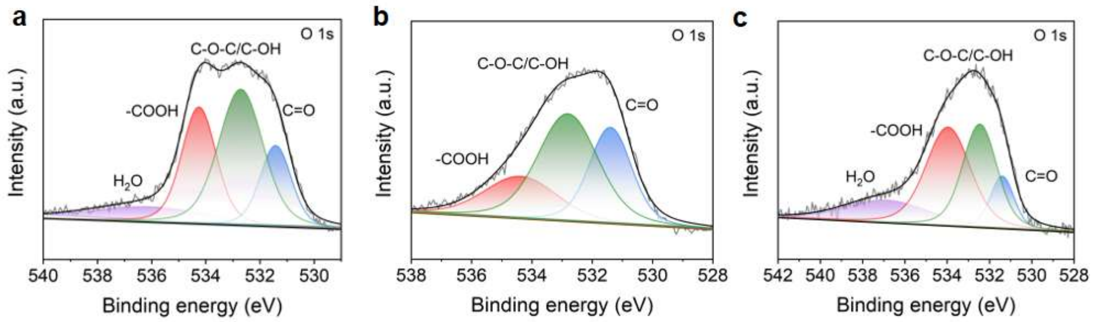

Fig. S7. High-resolution O 1s XPS spectra of (a) TMLC-600. (b) TMLC-800 (C) TMLC-900.

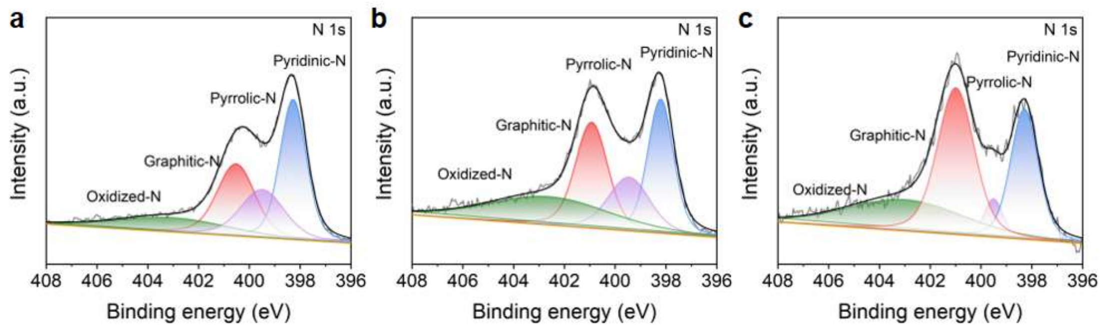

Fig. S8. High-resolution N 1s XPS spectra of (a) TMLC-600. (b) TMLC-800 (C) TMLC-900.

Table S2 Atomic elemental content of TMLCs.

Sample	C (at%)	N (at%)	O (at%)
TMLC-600	79.2	14.7	6.1
TMLC-700	79.5	15.5	5.0
TMLC-800	83.0	10.7	6.3
TMLC-900	89.0	6.2	4.8

Table S3 Carbon bonding analysis of TMLCs.

Binding Energy (eV)	Carbon Bonding	Relative Concentration (%)			
		TMLC-600	TMLC-700	TMLC-800	TMLC-900
284.8	C-C/C=C	62.66	47.39	55.00	51.55
286.2	C=N	18.35	22.40	27.80	18.00
287.6	C-O	8.21	14.20	11.93	12.23
290.2	O-C=O	10.78	15.92	5.26	18.22

Table S4 The proportion of different nitrogen doping configurations of TMLCs.

Sample	N-6 (%)	N-5 (%)	N-Q (%)	N-O (%)
TMLC-600	36.6	20.9	27.0	15.6
TMLC-700	33.4	28.0	17.7	20.9
TMLC-800	27.6	17.8	27.3	27.4
TMLC-900	27.0	5.3	40.5	27.2

Table S5 Oxygen bonding analysis of TMLCs.

Binding Energy (eV)	Oxygen Bonding	Relative Concentration (%)			
		TMLC-600	TMLC-700	TMLC-800	TMLC-900
531.4	C=O	17.59	30.43	29.95	11.31
532.3	C-OH/ C-O-C	41.69	54.95	47.28	31.82
534.0	COOH	27.71	30.43	22.78	39.58
536.4	H_2O	13.02	-	-	17.30

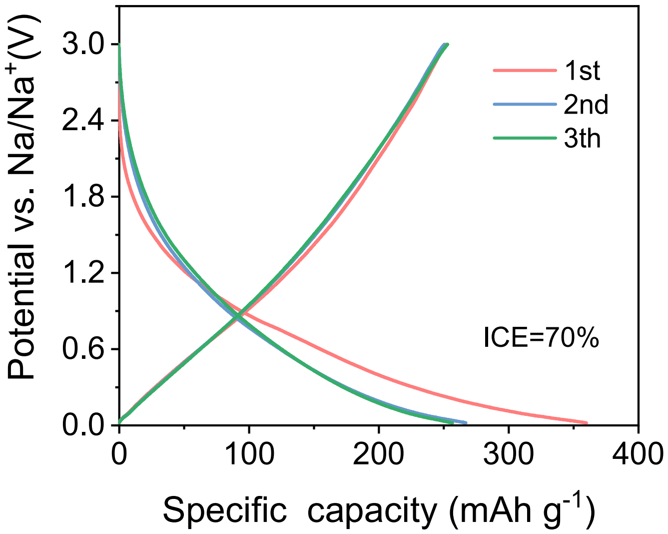

Fig. S9. GCD curves of the TMLC-700.

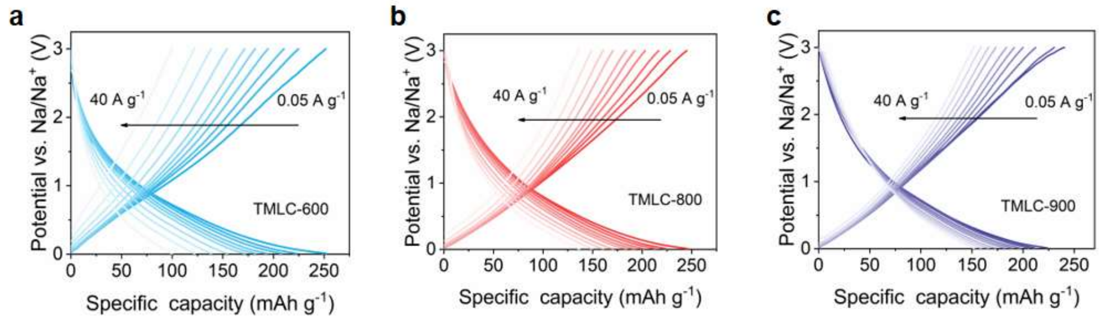

Fig. S10. GCD curves of (a) TMLC-600, (b) TMLC-800 and (c) TMLC-900.

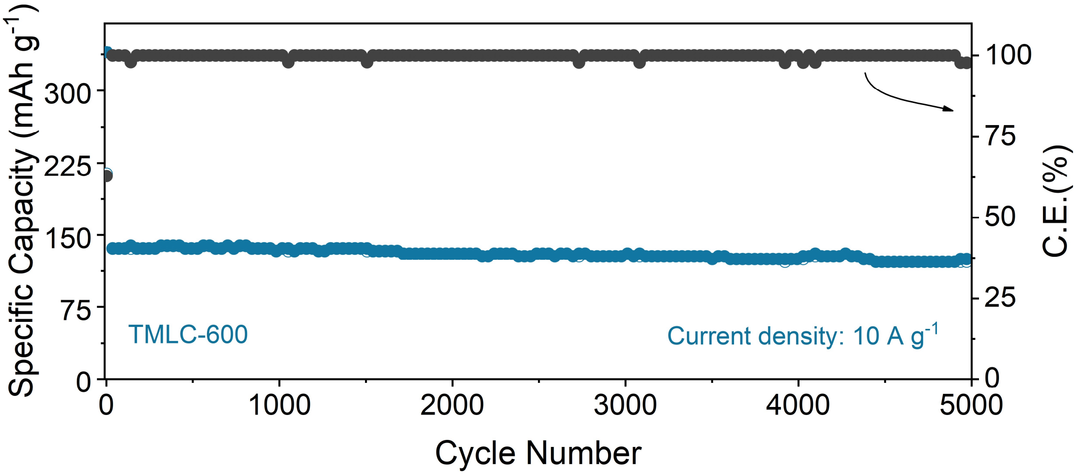

Fig. S11. Long-term GCD cycling stability of TMLC-600 at a current density of 10 A g^{-1}.

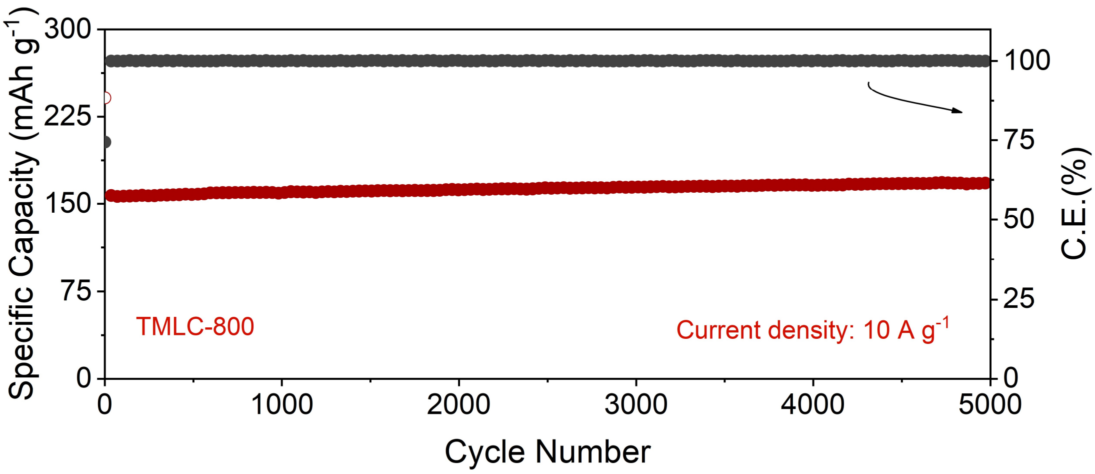

Fig. S12. Long-term GCD cycling stability of TMLC-800 at a current density of 10 A g^{-1}.

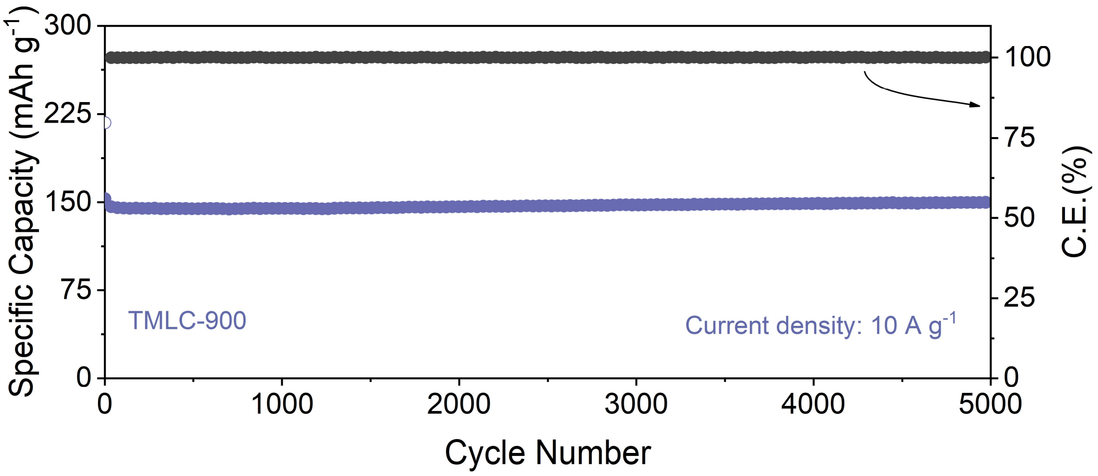

Fig. S13. Long-term GCD cycling stability of TMLC-900 at a current density of 10 A g^{-1}.

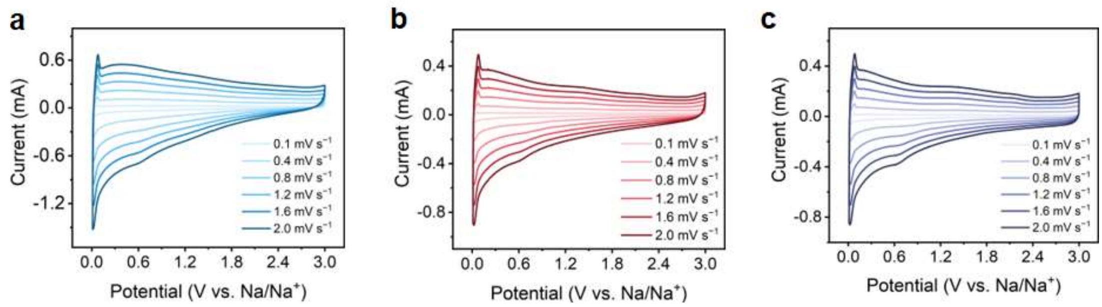

Fig. S14. CV curves at scan rates from 0.1 to 2 mV s^{-1} of (a) TMLC-600, and (b) TMLC-800 and (c) TMLC-900.

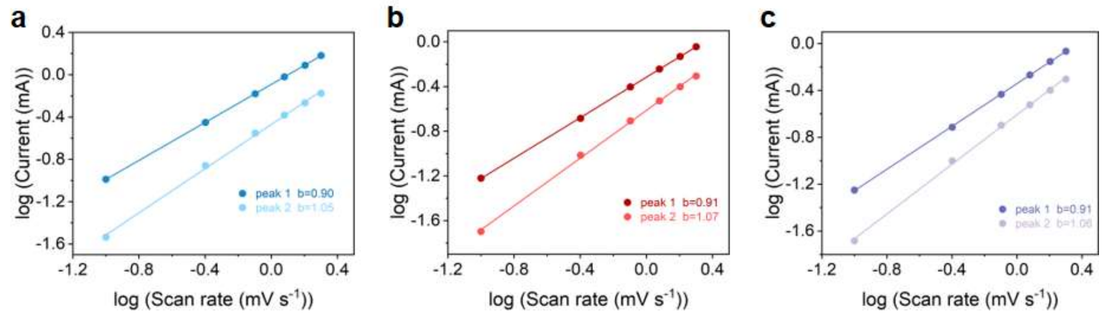

Fig. S15. The b values of (a) TMLC-600, (b) TMLC-800 and (c) TMLC-900.

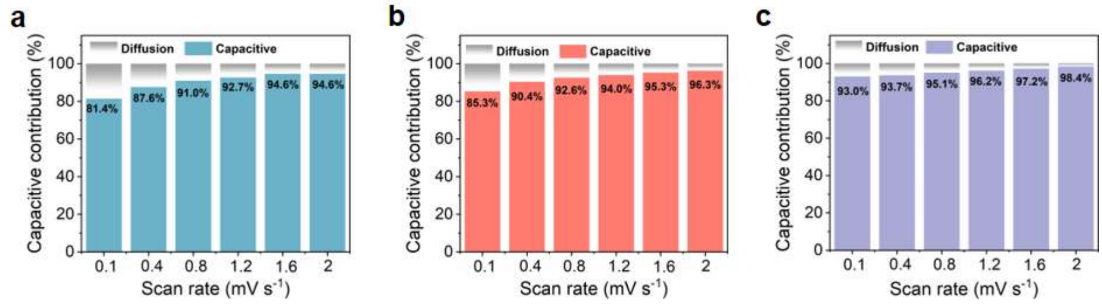

Fig. S16. Capacitive contributions at scan rates from 0.1 to 2 mV s^{-1} of (a) TMLC-600, and (b) TMLC-800 and (c) TMLC-900.

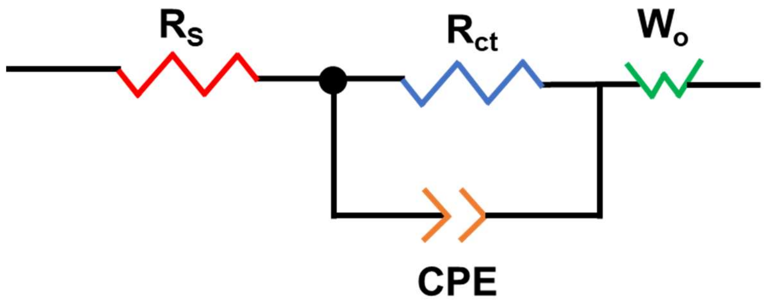

Fig. S17. The equivalent circuit model of EIS.

Table S6 The fitted values of circuit components of EIS.

Sample	Rs (ohm)	Rct (ohm)
TMLC-600	4.76	12.09
TMLC-700	3.79	9.48
TMLC-800	3.54	18.99
TMLC-900	6.75	7.22

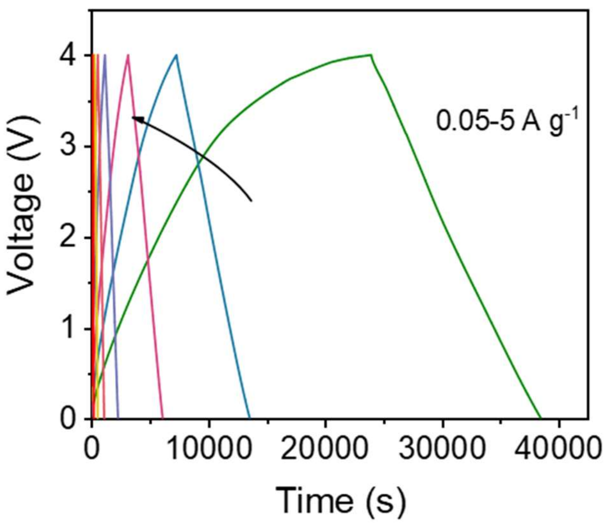

Fig. S18. The charge-discharge profiles of the SIHCs (TMLC-700//YP-80F) at different current densities.

Supplementary References

1. C. Bannwarth, S. Ehlert and S. Grimme, *J. Chem. Theory Comput.*, 2019, **15**, 1652-1671.
2. T. Lu and Q. Chen, *J. Comput. Chem.*, 2022, **43**, 539-555.
3. T. Lu and F. Chen, *J. Comput. Chem.*, 2012, **23**, 580-592.
4. W. Humphrey, A. Dalke and K. Schulten, *J. Mol. Graphics*, 1996, **14**, 33-38.
5. J. Liu, X. Qiu, S. Sun, B. Liu, Y. Tian, Y. Qin and X. Lin, *Green Chemistry*, 2024, **26**, 8020-8029.